Bioorganic & Medicinal Chemistry Letters 22 (2012) 96–101

Contents lists available at SciVerse ScienceDirect

Bioorganic & Medicinal Chemistry Letters

journal homepage: www.elsevier.com/locate/bmcl

5-(2-Amino-pyrimidin-4-yl)-1*H*-pyrrole and 2-(2-amino-pyrimidin-4-yl)-1,5,6,7-tetrahydro-pyrrolo[3,2-*c*]pyridin-4-one derivatives as new classes of selective and orally available Polo-like kinase 1 inhibitors

Michele Caruso [a], Barbara Valsasina [a], Dario Ballinari [a], Jay Bertrand [a], Maria Gabriella Brasca [a], Marina Caldarelli [a], Paolo Cappella [a], Francesco Fiorentini [b], Laura M. Gianellini [a], Alessandra Scolaro [a], Italo Beria [a,*]

[a] *Nerviano Medical Sciences srl, Business Unit Oncology, Viale Pasteur 10, 20014 Nerviano, (MI), Italy*
[b] *Accelera srl, Viale Pasteur 10, 20014 Nerviano, (MI), Italy*

ARTICLE INFO

Article history:
Received 13 September 2011
Revised 17 November 2011
Accepted 18 November 2011
Available online 23 November 2011

Keywords:
PLK1
Polo-like kinase
PLK2 and PLK3
Cell cycle
Cellular activity
Crystal structure

ABSTRACT

The discovery and characterization of two new chemical classes of potent and selective Polo-like kinase 1 (PLK1) inhibitors is reported. For the most interesting compounds, we discuss the biological activities, crystal structures and preliminary pharmacokinetic parameters. The more advanced compounds inhibit PLK1 in the enzymatic assay at the nM level and exhibit good activity in cell proliferation on A2780 cells. Furthermore, these compounds showed high levels of selectivity on a panel of unrelated kinases, as well as against PLK2 and PLK3 isoforms. Additionally, the compounds show acceptable oral bioavailability in mice making these inhibitors suitable candidates for further in vivo activity studies.

Mitotic cell cycle progression is tightly regulated through reversible covalent protein phosphorylation events coordinated by regulatory kinases, including members of the Polo subfamily.[1,2] Polo-like kinases (PLKs) are a group of highly conserved serine/threonine kinases with an important role in the mitosis process.[3,4] Currently, five members of the PLK family have been identified in humans (PLK1–5); among them, PLK1 is the best characterized and is recognized to be a key component of the cell cycle control machinery with important roles in the mitotic entry, centrosome duplication, bipolar mitotic spindle formation, transition from metaphase to anaphase, cytokinesis and maintenance of genomic stability.[5,6] PLK1 has been found to be overexpressed in a variety of tumors and has been shown to correlate with poor clinical outcomes.[7] Less clear is the functional role of the other PLK family members, especially those of PLK2 and PLK3 whose inhibition could cause toxicities associated with the nervous system or promote angiogenesis, respectively.[8,9] Thus, development of small molecules that selectively inhibit PLK1 could have reduced off-target effects.[10,11]

PLK1 inhibitors targeting the ATP binding pocket in the kinase domain or the PBD region of the enzyme are under development as potential anticancer agents.[10]

Recently, we disclosed the discovery and the optimization work of a series of 4,5-dihydro-1*H*-pyrazolo[4,3-*h*]quinazoline derivatives,[12–14] As part of our continuing effort in the search of novel PLK1 inhibitors, we report here the identification and optimization of both 5-(2-amino-pyrimidin-4-yl)-1*H*-pyrrole scaffold

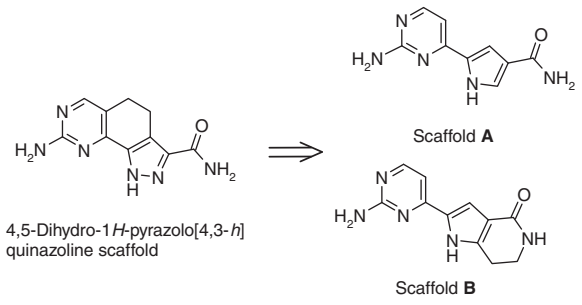

Figure 1. From pyrazolo-quinazoline to pyrimidinyl-pyrrole and pyrimidinyl-pyrrolo[3,2-*c*]pyridinone scaffolds.

* Corresponding author. Tel.: +39 331 581516; fax: +39 331 581347.
E-mail address: italo.beria@nervianoms.com (I. Beria).

0960-894X/$ - see front matter © 2011 Elsevier Ltd. All rights reserved.
doi:10.1016/j.bmcl.2011.11.065

A and 2-(2-amino-pyrimidin-4-yl)-1,5,6,7-tetrahydro-pyrrolo[3,2-*c*]pyridin-4-one scaffold **B**, that led to the identification of potent and selective ATP-competitive PLK1 inhibitors (Fig. 1). The chemical expansion, of the two scaffolds took advantage of the information acquired in the development of the 4,5-dihydro-1*H*-pyrazolo[4,3-*h*]quinazoline series, that related to the pyrrole and to the aminopyrimidine rings. In particular, three key moieties at the 1-position of the pyrrole ring and 2,5-disubstituted phenyl residues at the 2-amino-pyrimidin-4-yl template were identified as suitable appendixes to obtain selective and potent PLK1 inhibitors.

Synthesis of scaffold **A** was simply performed by hydrolysis of intermediate **1** and the subsequent reaction of the corresponding acid with 1-hydroxybenzotriazole ammonium salt ($HOBt{\cdot}NH_3$) and EDCI (Scheme 1).[15] Alkylation of the intermediate **1** at the 1-position of the pyrrole ring by reaction with the suitable halogen derivatives afforded the versatile intermediates **2–4**, that were used for subsequent introduction of the 2,5-disubstituted aniline residue at the 2-position of the pyrimidine ring, through two different pathways (Scheme 1). Compounds **7** and **9** were prepared by reacting esters **2** and **3** with 1-[3-iodo-4-(trifloromethoxy)phenyl]-4-methylpiperazine under Buchwald–Hartwig conditions catalyzed by $Pd_2(dba)_3$ and 4,5-bis(diphenylphosphino)-9,9-dimethylxanthene (Xantphos). Then, the ester function of intermediates **5** and **6** was converted to the corresponding amide to yield the compound **7** and the intermediate **8**, that was in turn converted to compound **9** by removal of the tetrahydropyranyl protecting group under acid conditions. Alternatively, compounds **13**, **14** and **15** were obtained transforming the 2-amino-4-pyrimidinyl derivative **4** to the corresponding 2-iodo derivative **10** via diazonium salt. Then, coupling of **10** with 5-bromo-2-(trifluoromethoxy)aniline, again exploiting Buchwald–Hartwig cross-coupling methodology, catalyzed by $Pd(OAc)_2$ and (±)-BINAP, afforded the bromo ester **11**, which was converted to the corresponding amide **12** in two steps, as previously reported. Finally, further palladium mediated C–N bond formation with the suitable piperazine derivatives, $Pd_2(dba)_3$ and 2-dicyclohexylphosphophino-2′-(*N*,*N*-dimethylamino)-biphenyl gave, directly or after removal of the protecting group, the final compounds **13, 14** and **15**, respectively.

Scaffold **B** and its derivatives were prepared starting from compound **16**.[16] Removal of Boc protecting group from compound **16** yielded directly scaffold **B**, while alkylation of **16** at the 1-position

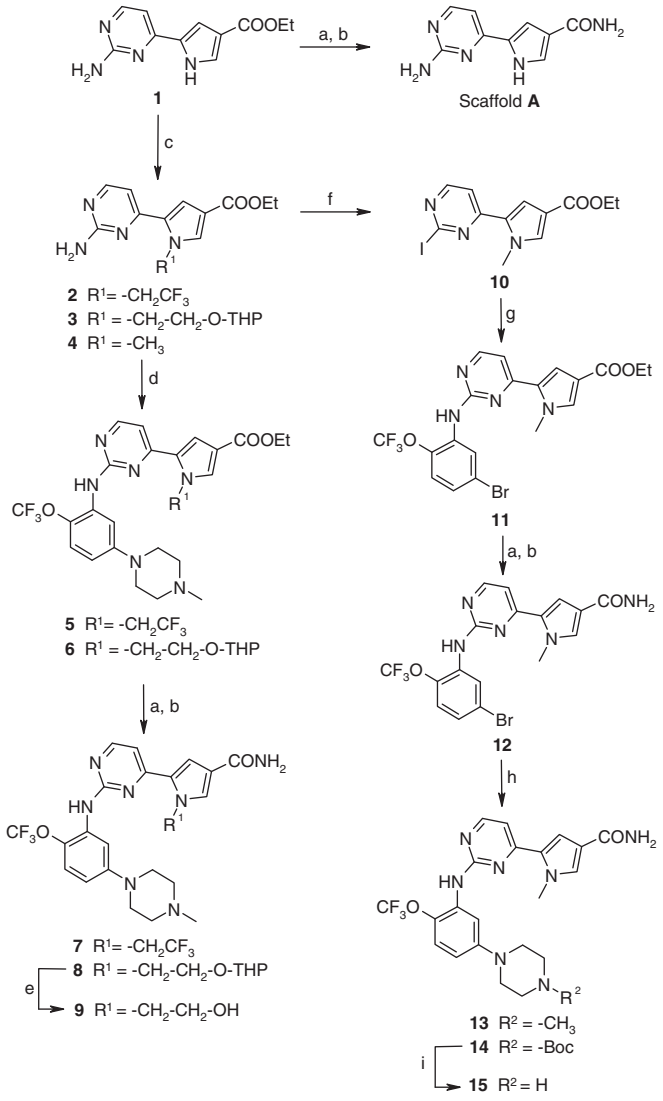

Scheme 1. Reagents and conditions: (a) 2 M KOH in EtOH, 80 °C, 3 h, quant.; (b) DMF/DCM 1:1 mixture, EDCI, $HOBt{\cdot}NH_3$, TEA, rt, 24 h, 60–90%; (c) THF/DMSO, NaH, R^1-I or R^1-Br, rt, 12 h, 70–82%; (d) 1-[3-iodo-4-(trifloromethoxy)phenyl]-4-methylpiperazine, $Pd_2(dba)_3$, Xantphos, Cs_2CO_3, 110 °C, 8 h, 50–75%; (e) PTSA, MeOH, rt, 6 h, 70%; (f) CsI, I_2, CuI, isopentyl nitrite, DME, 70 °C, 6 h, 25%; (g) $Pd(OAc)_2$, (±)-BINAP, K_2CO_3, 5-bromo-2-(trifluoromethoxy)aniline, DMF, 80 °C, 6 h, 52%; (h) 1-methylpiperazine or *N*-Boc-piperazine, $Pd_2(dba)_3$, 2-dicyclohexylphosphophino-2′-(*N*,*N*-dimethylamino)-biphenyl, $LiN(TMS)_2$/THF, 80 °C, 8 h, 50–60%; (i) 4 M HCl in dioxane, rt, 6 h, 66%.

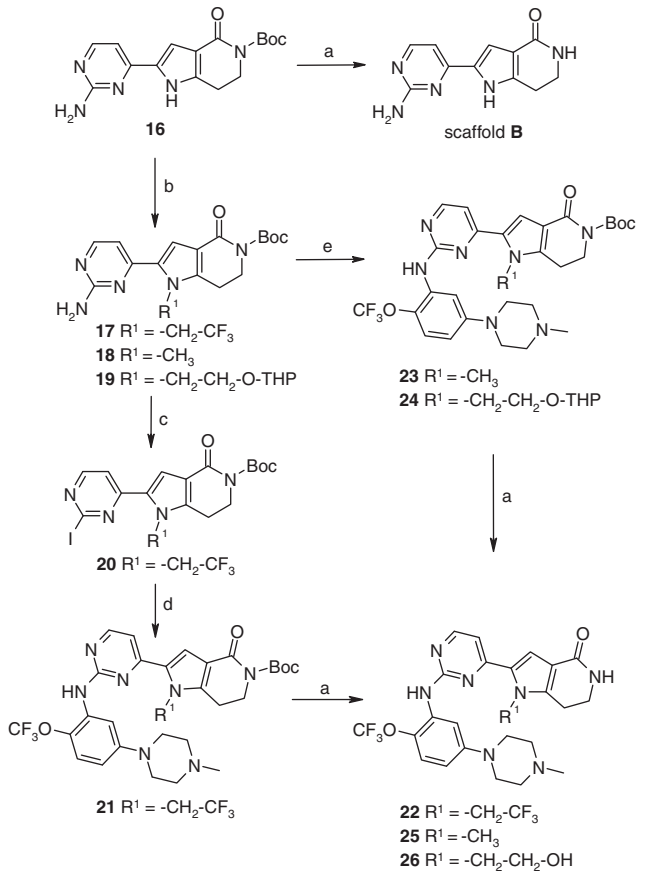

Scheme 2. Reagents and conditions: (a) 4 M HCl in dioxane, rt, 6 h, 30–98%; (b) DMF, Cs_2CO_3, R^1-I or R^1-Br, rt, 4 h, 70-90%; (c) CsI, I_2, CuI, isopentyl nitrite, DME, 80 °C, 4 h, 35%; (d) $Pd(OAc)_2$, (±)-BINAP, K_2CO_3, 5-(4-methylpiperazin-1-yl)-2-(trifuoromethoxy)aniline, DMF, 80 °C, 2 h, 25%; (e) 1-[3-iodo-4-(trifloromethoxy)phenyl]-4-methylpiperazine, $Pd_2(dba)_3$, Xantphos, Cs_2CO_3, dioxane, reflux, 2 h, 75–85%.

of the pyrrole ring by reaction with the suitable halogen derivatives afforded versatile intermediates **17**–**19** (Scheme 2).[15] Two synthetic approaches were exploited to convert intermediates **17**–**19** to final compounds **22**, **25** and **26**. The first approach foresaw the substitution of the amino group of intermediate **17** with iodine through diazononium salt formation followed by Buchwald–Hartwig cross-coupling of iodo derivative **20** with 5-(4-methyl-piperazin-1-yl)-2-(trifluoromethoxy)aniline catalyzed by $Pd(OAc)_2$ and (±)-BINAP to yield the compound **21**. Finally, removal of the Boc protecting group afforded compound **22**. In the second synthetic approach, compounds **25** and **26** were obtained in a shorter way by reacting the protected intermediates **18** and **19** with the 2-trifluoromethoxy-iodobenzene derivatives using $Pd_2(dba)_3$ and Xantphos and then removing the protecting groups from intermediates **23** and **24** with trifluoroacetic acid.[15]

Compounds were tested in the biochemical assay against PLK1–3, CDK2/A and Aur-A kinases and their activity in cell proliferation assay was evaluated on A2780 cell lines. In both series, the introduction of selected R^1 and 5-(4-methyl-piperazin-1-yl)-2-(trifluoromethoxy)aniline residues transformed the inactive scaffolds **A**

Table 1
SAR of 5-(2-Amino-pyrimidin-4-yl)-1*H*-pyrrole derivatives

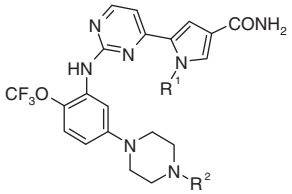

Compound	R^1	R^2	PLK1 IC_{50}[a] (μM)	PLK2 IC_{50}[a] (μM)	PLK3 IC_{50}[a] (μM)	CDK2/A IC_{50}[a] (μM)	Au-AIC_{50}[a] (μM)	A2780 IC_{50}[a] (μM)
Scaffold **A**			>10	nd	nd	>10	>10	nd
13	$-CH_3$	$-CH_3$	0.015	>10	>10	>10	>10	0.360
7	$-CH_2-CF_3$	$-CH_3$	0.018	>10	>10	>10	>10	0.109
15	$-CH_3$	H	0.018	>10	>10	>10	>10	0.610
9	$-(CH_2)_2-OH$	$-CH_3$	0.151	>10	>10	>10	>10	2.531
8	$-(CH_2)_2-O-THP$	$-CH_3$	0.272	>10	>10	>10	>10	6.690
14	$-CH_3$	$-C(O)OC(CH_3)_3$	>10	>10	>10	>10	>10	4.513

[a] Values are means of three experiments. Standard deviation is <20%. nd = not determined.

Table 2
SAR of 2-(2-amino-pyrimidin-4-yl)-1,5,6,7-tetrahydro-pyrrolo[3,2-*c*]pyridin-4-one derivatives

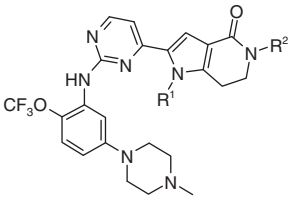

Compound	R^1	R^2	PLK1 IC_{50}[a] (μM)	PLK2 IC_{50}[a] (μM)	PLK3 IC_{50}[a] (μM)	CDK2/A IC_{50}[a] (μM)	Aur-A IC_{50}[a] (μM)	A2780 IC_{50}[a] (μM)
Scaffold **B**			1.131	nd	nd	0.219	>10	1.53
25	$-CH_3$	H	0.009	>10	>10	>10	>10	0.037
22	$-CH_2-CF_3$	H	0.028	>10	>10	>10	>10	0.062
26	$-(CH_2)_2-OH$	H	0.102	>10	>10	>10	>10	0.722
23	$-CH_3$	$-C(O)OC(CH_3)_3$	0.817	>10	>10	>10	>10	0.176

[a] Values are means of three experiments. Standard deviation is <20%.

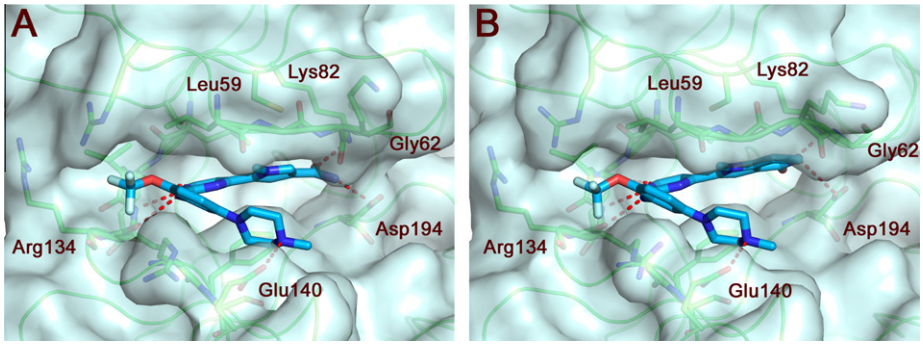

Figure 2. Crystal structure of inhibitors **13** (panel A) and **25** (panel B) bound to PLK1. Hydrogen bonds are shown as red dashed lines (PBD 4A4L and 4A4O, respectively).

Table 3
Kinase profile of compounds **13** and **25** on a larger kinase panel

Enzyme	Compound **13** IC_{50}[a] (μM)	Compound **25** IC_{50}[a] (μM)
PLK1	0.015	0.009
CK2	0.951	0.420
FLT3	nd	0.659
Other kinases[b]	>10	>10

[a] Values are means of three experiments. Standard deviation is <20.
[b] For the list of kinases, see Ref. 18.

Table 4
Activity of compounds **13** and **25** on different cell lines

Cell lines	Tumor types	Compound **13** IC_{50}[a] (μM)	Compound **25** IC_{50}[a] (μM)
A375	Melanoma	0.386	0.027
HCT-116	Colon	0.520	0.032
LNCaP	Prostate	0.280	0.026
MDA-MB-468	Breast	0.624	0.041
K-562	Leukemia	0.590	0.060
MOLM-13	Leukemia	0.201	0.021
MOLT-4	Leukemia	0.253	0.017
SUP-M2	Lymphoma	0.647	0.053

[a] Values are means of two experiments. Standard deviation is <20%.

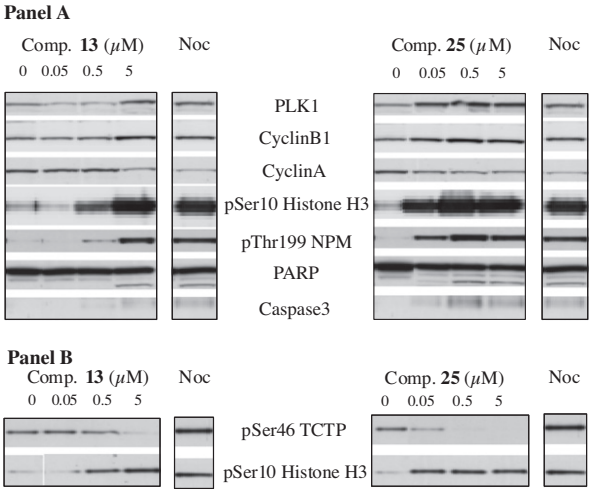

Figure 4. Western Blot analysis of compounds **13** and **25** on A2780 cell lines. Cells were treated with the compounds at three different doses (0.05 μM, 0.5 μM and 5 μM) for 24 h (Panel **A**) or for 1 h (Panel **B**). Nocodazole (Noc) treated cells are used as positive control. PLK1 specific marker (pSer46 TCTP), as well as mitotic markers (pSer10 Histone H3 and pThr199 NPM) and apoptosis markers were evaluated.

and **B** into potent and selective PLK1 inhibitors, as outlined in Tables 1 and 2. These results are in agreement with what we found in the past for the 4,5-dihydro-1*H*-pyrazolo[4,3-*h*]quinazoline series.[12–14] Also the loss of activity of compound **14**, wherein the basicity of the 4-N of the piperazine appendix is destroyed by formation of a carbamate bond, is in agreement with the previously published results.[12,13] Among the most interesting new inhibitors, compound **13** was selected as representative of the class for a deeper characterization.

The trend of activity observed in the 5-pyrimidin-4-yl-1*H*-pyrrole series was also found in the 2-pyrimidin-4-yl-1,5,6,7-tetrahydro-pyrrolo[3,2-*c*]pyridin-4-one series. Thus, while scaffold **B** resulted poorly active against PLK1 with high cross-reactivity versus CDK2/A (Table 2), the introduction of the key residues at the pyrrole and at the pyrimidine nucleous on the scaffold, as in compounds **22**, **23**, **25**, and **26**, led to the loss of CDK2/A cross reactivity and a remarkable improvement of the potency against PLK1, associated to a significant cellular activity. The best inhibitor of the series resulted the compound **25** that showed more than 140-fold increase in the PLK1 activity and more than 40-fold improvement of the cellular cytotoxicity.

In order to characterize the binding modes for the two different chemical classes, crystal structures of compounds **13** and **25** were solved in complex with PLK1 to 2.35 and 2.70 Å resolution, respectively.[17] The activation loop of PLK1 in the crystals showed a DFG-in conformation indicative of an active form of the kinase. As expected, the two compounds bind in the ATP-pocket making similar interactions with the protein; furthermore, these interactions are similar to those recently reported for the related compound NMS-P937.[14] In fact, both inhibitors make donor–acceptor–donor interactions with the PLK1 hinge residues Glu131 and Cys133, both make hydrogen bonds with Lys182 and Asp194 and both make a polar interaction with the sidechain of Glu140. In addition, both inhibitors bind their 2-trifluoromethoxy groups in the pocket formed by Arg57 and the hinge segment Leu132–Cys133–Arg134 and multipolar interactions are present between the fluorine atoms from each inhibitor and the backbone carbonyl of Arg134 (Fig. 2). One significant difference between the two structures is the presence of the pyridin-4-one ring in **25** that is situated underneath the glycine-rich loop residues Lys61 and Gly62. In contrast, since **13** lacks a similar moiety the corresponding region under the glycine-rich loop is left vacant.

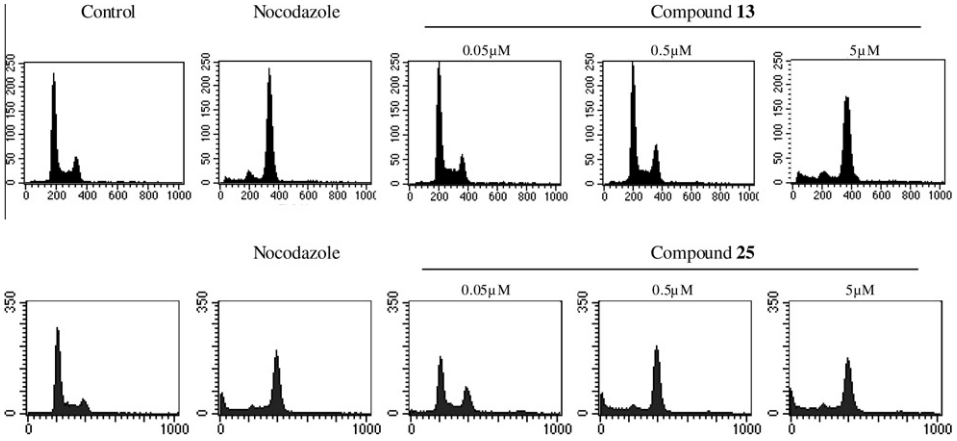

Figure 3. Flow cytometry analysis on A2780 cell lines treated for 24 h with 0.05, 0.5 and 5 μM of compounds **13** and **25**, respectively. Nocodazole was used as a positive control.

Table 5
In vitro ADME parameters of the selected compounds **13** and **25**

Compound	Permeability		Metabolic stability		Solubility pH 7 (μM)
	Caco-2 *P*app (10^{-6} cm/s)	PAMPA[a] *P*app (10^{-6} cm/s)	Cl_{int}[b] (mL/min/kg) rat hepatocytes (1 μM)	Cl_{int} (mL/min/kg) HLM[c] (1 μM)	
13	High	50.00	408	14.90	174
25	Moderate	5.79	—	16.50	163

[a] Parallel artificial membrane permeability.
[b] Intinsic clearance.
[c] Human liver microsomes.

Table 6
In vivo pharmacokinetic parameters ± standard deviation of selected compounds **13** and **25** in Bulb Nu/Nu mice[a]

Compound	PK data (iv), dose: 10 mg/kg				PK data (po), dose: 10 mg/kg			
	AUC_{∞} (μM·h)	CL (mL/min/kg)	V_{ss} (L/kg)	$t_{1/2}$ (h)	C_{max}[d] (μM)	AUC_{∞}[e] (μM·h)	$t_{1/2}$[f] (h)	*F* (%)[g]
13[b]	5.41 ± 2.18	74.70 ± 35.20	2.50 ± 0.52	0.65 ± 0.28	0.76 ± 0.22	1.92 ± 0.43	1.70 ± 0.70	36
25[c]	5.78 ± 3.10	66.40 ± 27.60	2.49 ± 0.80	0.52 ± 0.15	0.76 ± 0.09	2.38 ± 0.06	1.40 ± 0.23	52

[a] *n* = 3 animals per study.
[b] Dosed as trifluoroacetate salt in dextrose.
[c] Dosed as free base in 50% PEG 400/glucosate (iv); as free base in 0.5% methocel (po).
[d] Maximum plasma concentration.
[e] Area under the curve.
[f] Terminal half-life.
[g] Bioavailability.

The selected compounds **13** and **25**, belonging to the two different chemical classes were then further screened against a wide kinase panel (39 kinases),[18] where they confirmed the high selectivity profile (Table 3). From this screening compound **13** was found to cross react only with CK2 kinase (IC_{50} = 0.951 μM), while compound **25** cross reacted with both CK2 and FLT3 (IC_{50} = 0.420 μM and IC_{50} = 0.659 μM, respectively). Cellular activity was also evaluated in a small panel of cell lines from tumors of different origin. Both compounds showed good activity in all tested cell lines with a higher potency of compound **25** with respect to **13** (Table 4).

The mechanism of action of compounds **13** and **25** was evaluated by fluorescence activated cell sorting analysis (FACS) and by Western Blot analysis in A2780 cell lines. In agreement with a PLK1 mechanism, a clear cell cycle block, with cell accumulation in the G_2–M phase, was indeed shown by FACS analysis after 24 h treatment with both selected inhibitors (Fig. 3). The PLK1 mechanism was also demonstrated by Western Blot. After 24 h cell treatment the modulation of different cell cycle markers including cyclin B1, cyclin A, phospho Ser10 histone H3, phospho Thr 199 Nucleophosmin and apoptotic markers such as PARP cleavage and caspase3 activation were evaluated. An increase in phosho Ser10 histone H3 and phosho Thr 199 Nucleophosmin signals, in agreement with a mitotic block mechanism, was observed for both inhibitors in a dose dependent manner with apoptosis induction, detected by PARP cleavage and Caspase 3 activation, at higher tested doses (Fig. 4 Panel A). Additionally, 1 h treatment of cells with both compounds **13** and **25** showed down-regulation of phosphorylation of the direct PLK1 substrate Translationally Controlled Tumor Protein (TCTP) as well as increased pSer 10 histone H3 levels (Fig. 4 Panel B). This behavior clearly differentiate PLK1 inhibitors form nocodazole treated cells where increase of pSer10 histone H3 is correlated with increase in pSer46 TCTP signal and indicative of a different mechanism of mitotic block.[19]

The selected compounds were further profiled for Absorption, Distribution, Metabolism and Excretion (ADME) properties and for pharmacokinetic characteristics. As reported in Table 5, both inhibitors show similar profiles with compound **13** showing a slightly better permeability profile, both in the PAMPA assay and in the caco-2 assay. Both compounds also show good solubility and good metabolic stability, especially in human liver microsomes.

Pharmacokinetic properties were evaluated in male Balb Nu/Nu, Harlan mice at 10 mg/kg following intravenous (iv) and oral (po) administration (Table 6). After iv dosing both compounds **13** and **25** showed similar behavior, with medium/high clearance and a volume of distribution about 4-fold the total body water, suggesting a good distribution of the compounds into tissues. After oral administration both compounds exhibited the same C_{max} value (0.76 μM), that for compound **13** is reached after 30 min. post-dosing, while for compound **25** after 90 min. post-dosing. Most importantly, the two compounds showed good oral bioavailability that, for compound **25** was found to reach 52%.

In summary we have reported here the development of two new chemical classes that led to the identification of two lead compounds **13** and **25**; both compounds demonstrated high activity on PLK1 and good selectivity versus a wide panel of kinases, as well as versus the PLK2 and PLK3 isoforms. The two new inhibitors possess good pharmacokinetic profile and good oral bioavailability in mouse. In particular, compound **25** showed 52% oral bioavailability that, taken together with the good activity in the cellular proliferation assay (IC_{50} = 37 nM on A2780) makes it a good candidate for further in vivo activity studies.

Acknowledgments

A particular thank to Roberto Bossi for his work on the crystal structures. We also thank the group of Assay Development and Biochemical Screening for the biochemical assay on kinase panel, Walter Ceccarelli and Gabriele Fachin for the compounds' synthesis, the Biochemistry Laboratory for protein production, Daniele Donati and Eduard R. Felder for their useful comments on the manuscript.

References and notes

1. Glover, D. M.; Hagan, I. M.; Tavares, A. A. *Genes Dev.* **1998**, *12*, 3777.
2. Nigg, E. A. *Curr. Opin. Cell Biol.* **1998**, *10*, 776.
3. Barr, F. A.; Sillje, H. H.; Nigg, E. A. *Nat. Rev. Mol. Cell Biol.* **2004**, *5*, 429.
4. Petronczki, M.; Lénárt, P.; Peters, J. M. *Dev. Cell* **2008**, *14*, 646.
5. van Vugt, M. A.; van de Weerdt, B. C.; Vader, G.; Janssen, H.; Calafat, J.; Klompmaker, R.; Wolthuis, R. M.; Medema, R. H. *J. Biol. Chem.* **2004**, *279*, 36841.

6. Qian, Y. W.; Erikson, E.; Taieb, F. E.; Maller, J. L. *Mol. Biol. Cell.* **2001**, *12*, 1791.
7. (a) Weichert, W.; Schmidt, M.; Gekeler, V.; Denkert, C.; Stephan, C.; Jung, K.; Loening, S.; Dietel, M.; Kristiansen, G. *Prostate* **2004**, *60*, 240; (b) Weichert, W.; Kristiansen, G.; Schmidt, M.; Gekeler, V.; Noske, A.; Niesporek, S.; Dietel, M.; Denkert, C. *World J. Gastroenterol.* **2005**, *11*, 5644; (c) Takai, N.; Hamanaka, R.; Yoshimatsu, J.; Miyakawa, I. *Oncogene* **2005**, *24*, 287; (d) Wolf, G.; Elez, R.; Doermer, A.; Holtrich, U.; Ackermann, H.; Stutte, H. J.; Altmannsberger, H. M.; Rübsamen-Waigmann, H.; Strebhardt, K. *Oncogene* **1997**, *14*, 543; (e) Knecht, R.; Elez, R.; Oechler, M.; Solbach, C.; von Ilberg, C.; Strebhardt, K. *Cancer Res.* **1999**, *59*, 2794; (f) Schmit, T. L.; Zhong, W.; Setaluri, V.; Spiegelman, V. S.; Ahmad, N. *J. Invest. Dermatol.* **2009**, *129*, 2843.
8. Kauselmann, G.; Weiler, M.; Wulff, P.; Jessberger, S.; Konietzko, U.; Scafidi, J.; Staubli, U.; Bereiter-Hahn, J.; Strebhardt, K.; Kuhl, D. *EMBO J.* **1999**, *18*, 5528.
9. Andrysik, Z. et al *Nucleic Acids Res.* **2010**, *38*, 2931.
10. Strebhardt, K. *Nat. Rev. Drug Disc.* **2010**, *9*, 643.
11. Medema, R. H.; Lens, S. M.; Voest, E. E. *Nat. Rev. Cancer* **2010**, *10*, 825.
12. Beria, I.; Ballinari, D.; Bertrand, J. A.; Borghi, D.; Bossi, R. T.; Brasca, M. G.; Cappella, P.; Caruso, M.; Ceccarelli, W.; Ciavolella, A.; Cristiani, C.; Croci, V.; De Ponti, A.; Fachin, G.; Ferguson, R. D.; Lansen, J.; Moll, J. K.; Pesenti, E.; Posteri, H.; Perego, R.; Rocchetti, M.; Storici, P.; Volpi, D.; Valsasina, B. *J. Med. Chem.* **2010**, *53*, 3532.
13. Beria, I.; Valsasina, B.; Brasca, M. G.; Ceccarelli, W.; Colombo, M.; Cribioli, S.; Fachin, G.; Ferguson, R. D.; Fiorentini, F.; Gianellini, L. M.; Giorgini, M. L.; Moll, J. K.; Posteri, H.; Pezzetta, D.; Roletto, F.; Sola, F.; Tesei, D.; Caruso, M. *Bioorg. Med. Chem. Lett.* **2010**, *20*, 6489.
14. Beria, I.; Bossi, R. T.; Brasca, M. G.; Caruso, M.; Ceccarelli, W.; Fachin, G.; Fasolini, M.; Forta, B.; Fiorentini, F.; Pesenti, E.; Pezzetta, D.; Posteri, H.; Scolaro, A.; Re Depaolini, S.; Valsasina, B. *Bioorg. Med. Chem. Lett.* **2011**, *21*, 2969.
15. Beria, I.; Brasca, M. G.; Caruso, M.; Caldarelli, M.; Ceccarelli, W.; Posteri, H.; Patent WO 2009040399, **2009**.
16. Vanotti, E.; D'Alessio, R.; Tibolla, M.; Varasi, M.; Montagnoli, A.; Santocanale, C.; Orsini, P.; Pillan, A.; Patent WO 2005014572, **2005**.
17. Coordinates of the PLK1 complexes with compounds **13** and **25** have been deposited in the Protein Data Base under accession code 4A4L and 4A4O, respectively.
18. The kinase panel includes c-ABL, AKT1, Aur-B, BRK, CDC7, CDK1/B, CDK2/E, CDK4/D1, CDK5/P25, CHK1, CK2, EGFR1, ERK2, FGFR1, FLT3, GSK3β, IGFR1, IKK2, IR, JAK2, KIT, LCK, MAP-KAPK2, MET, MPS1, MST4, NEK6, NIM, P38α, PAK4, PDGFR, PDK1, PKAα, PKCβ, RET, SULU1, TRKA, VEGFR2,and VEGFR3.
19. Cucchi, U.; Gianellini, L. M.; De Ponti, A.; Sola, F.; Alzani, R.; Patton, V.; Pezzoni, A.; Troiani, S.; Saccardo, M. B.; Rizzi, S.; Giorgini, M. L.; Cappella, P.; Beria, I.; Valsasina, B. *Anticancer Res.* **2010**, *30*, 4973.